

ROUGH PREDICTION OF OSCILLATIONS BY COMPUTING MAXIMAL INSTABILITY

Zoran Rajilić*, Dragana Malivuk Gak

University of Banja Luka, Faculty of Natural Sciences, Mladena Stojanovića 2,
Banja Luka, Republic of Srpska, Bosnia and Herzegovina

*Corresponding author: ZoranRajilic@netscape.net

Abstract: We use Newton's second law of motion assuming combination chaos with stochasticity. For a measured time series, one can compute appropriate force and then better understand and roughly predict the behavior of the observed complex system. The force parameter describing instability is of the highest importance. We consider some mechanical experiments and the average global temperature.

Keywords: chaos, stochasticity, instability, earthquake, global temperature.

1. INTRODUCTION

It is no secret that throughout history, the laws of physics have often been attempted to be applied to systems such as society, economics, etc. In 1994, Dirk Helbing proposed a social force model for pedestrians, using Newton's second law. There are readjusting force (determined by the difference between desired walking speed and actual velocity), repulsion from borders, mutual repulsion between moving pedestrians and fluctuating force (accounting for non-predictable individual behavior). Force in this model is a measure of the internal motivation of the individual to perform a certain movement. An unexpected result is found—more stochasticity does not always correspond to more disorder in the system [1,2]. Force in the social impact theory describes the social influence of individuals persuading and supporting others [3]. Tomaš Zeithamer describes the time dependence of the price of goods using Newton's second law with damping force [4].

Complex systems are hardly predictable because of stochastic processes and sensitivity to initial conditions and force parameters. We will show that the exceptional instability in a short time interval makes possible the rough prediction of future oscillations. Our basic assumptions here are (i) applicability of Newton's second law on non-mechanical as well as mechanical systems and (ii) the combination chaos (short-term predictability) with stochasticity (unpredictability) [5].

We aim to improve understanding and rough prediction of complex systems by making an accurate transformation of experimental data to the force parameters as functions of discrete time.

First, we consider the artificial time series and investigate the influence of very large instability, in a short time interval, on the future-driven nonlinear oscillations which are occasionally damped and amplified. Then our approach to measured time series is explained. Finally, we apply the proposed method to the results of mechanical experiments, important in the

investigation of earthquakes, and the annual average global temperature.

2. ARTIFICIAL TIME SERIES

Nonlinear, driven and damped, or amplified, oscillations of a particle of unit mass we describe by the following differential equation of motion.

$$\frac{dv}{dt} = az + a_2z^2 + a_3z^3 + bv + w + \sum_{i=2}^6 c_i \cos \frac{6.28t}{i} \quad (1)$$

where

$$v = \frac{dz}{dt} \quad (2)$$

We assume that force parameters (a, a_2, a_3, b, w, c_i) are formed as

$$R_1 + g(t) + R_2f(t); \quad R_1, R_2 = const.$$

where $g(t)$ is a regular function of time and $f(t)$ is fluctuating function of time with values between -1 and 1 . We will perform computations with five different realizations of $f(t)$ (figure 1-5). If $a > 0$, oscillations are unstable. If we set the parameter a as

$$a = \dots + Qe^{-\kappa(t-t_0)^2}; \quad Q > 0, \kappa \gg 1,$$

then instability of level Q is located in a short time interval around t_0 . Large instability in that short interval causes a large change of $z(t)$ in the future (figure 1-7). To have a large delayed effect, the level of stochasticity is very important (Figs. 6, 7).

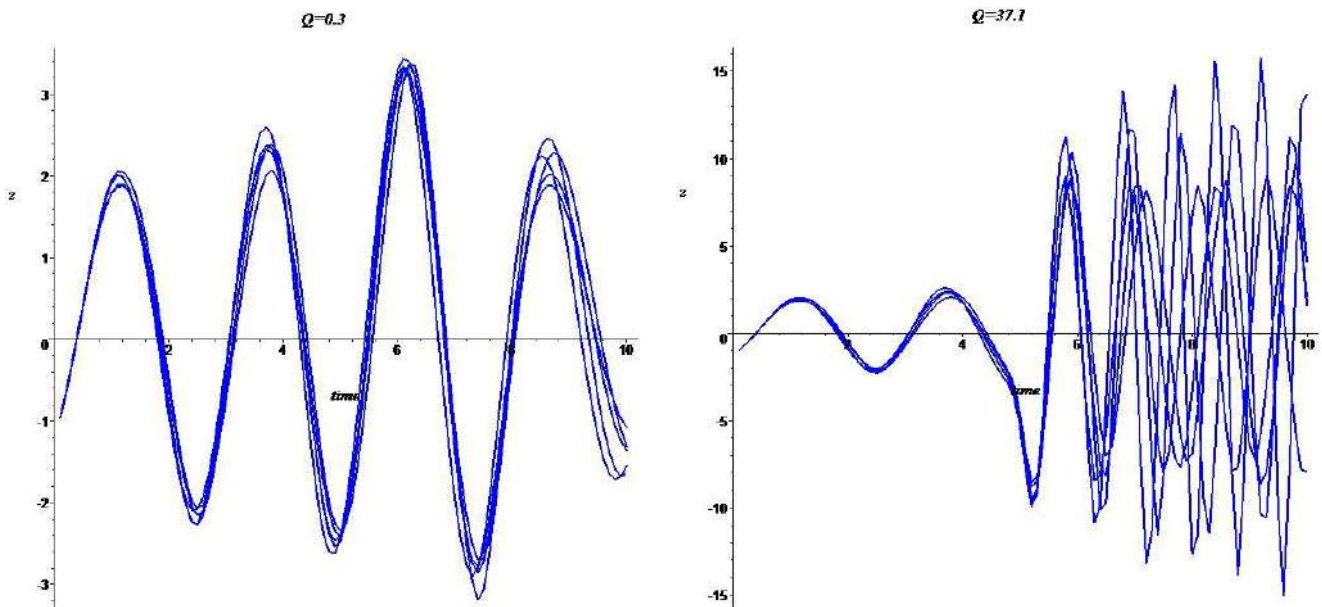


Figure 1. Solution of differential equation of motion (1) for $Q = 0.3$ (left) and 37.1 (right). Here $z(0) = -1.2, v(0) = 2.0, a = -4.5 + 1.4f(t) + Qe^{-17(t-5)^2}, a_2 = 0.5 + 0.3f(t), a_3 = -0.4 + 0.2f(t), b = -0.04 + 0.03f(t), w = -0.2 + 0.2f(t), c_2 = -0.8 + 0.6f(t), c_3 = 1.2 + 0.7f(t), c_4 = -1.1 + 0.5f(t), c_5 = 1.2 + 0.9f(t), c_6 = 0.8 + 0.6f(t)$. High positive parameter a (instability) near $t = 5$ causes very large uncertainty, amplitude and frequency in the future ($t > 7$).

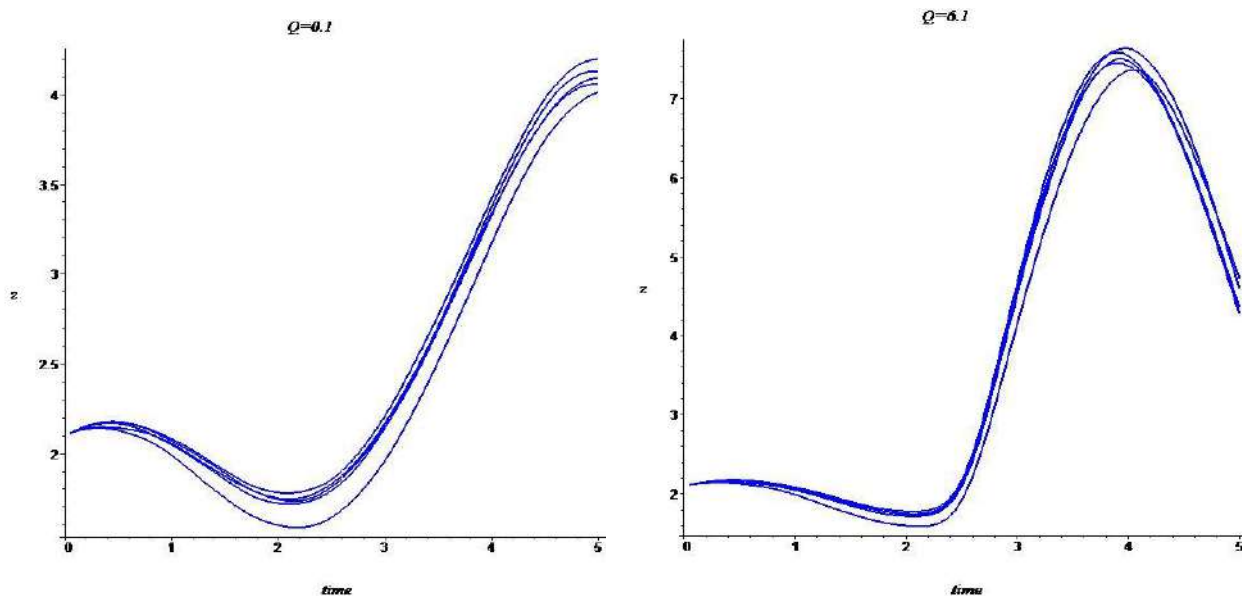


Figure 2. Solution of differential equation of motion (1) for $Q = 0.1$ and 6.1 . Here $z(0) = 2.1, v(0) = 0.3, a = -0.1 + 0.1f(t) + Qe^{-17(t-2.5)^2}, a_2 = 0.01 + 0.003f(t), a_3 = -0.02 + 0.01f(t), b = -0.4 + 0.03f(t), w = 0.5 + 0.4f(t), c_2 = 0.1 + 0.15f(t), c_3 = 0.1 + 0.1f(t), c_4 = 0.1 + 0.2f(t), c_5 = -0.1 + 0.1f(t), c_6 = -1.0 + 0.2f(t)$.

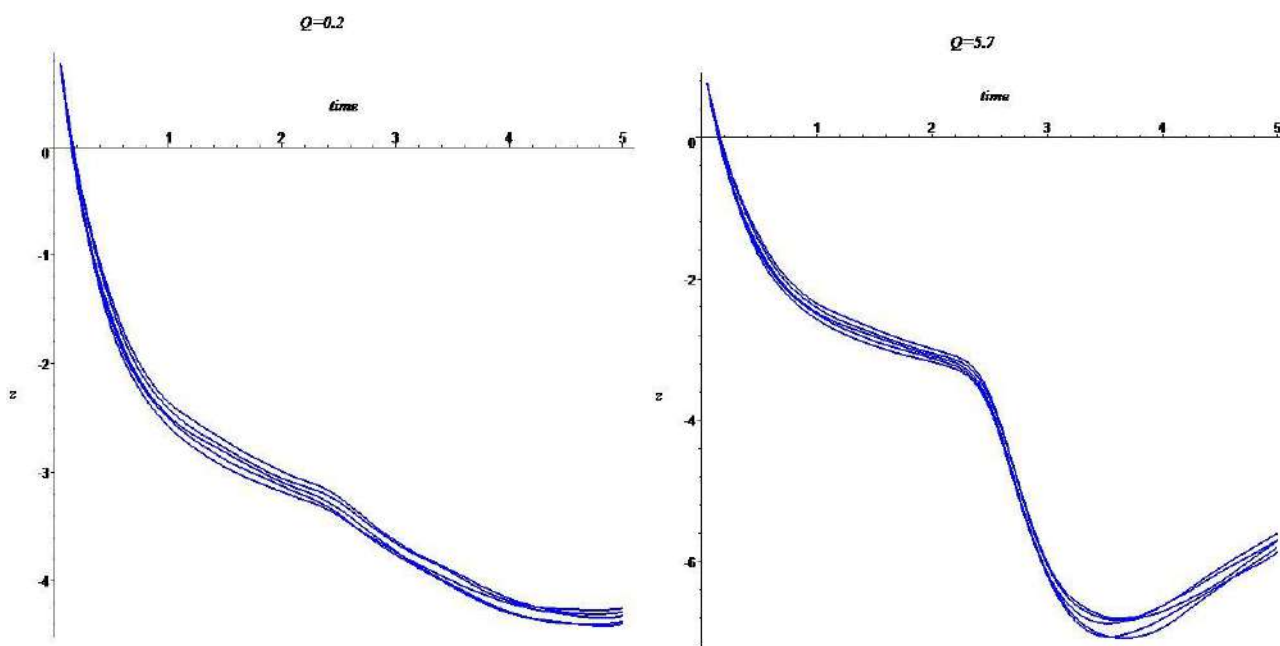


Figure 3. Solution of differential equation of motion (1) for $Q = 0.2$ and 5.7 . Here $z(0) = 1.2, v(0) = -9.3, a = -0.1 + 0.1f(t) + Qe^{-17(t-2.5)^2}, a_2 = 0.03 + 0.004f(t), a_3 = -0.01 + 0.01f(t), b = -2.4 + 0.8f(t), w = -1.5 + 0.1\sin(5.4t - 0.9) + 0.7f(t), c_2 = -0.1 + 0.3\sin(7.4t - 0.9) + 0.2f(t), c_3 = -0.2 - 0.7\sin(3.6t - 0.1) + 0.1f(t), c_4 = -0.3 + 0.2f(t), c_5 = 0.4 + 0.3\sin(8.4t - 0.5) + 0.2f(t), c_6 = 1.0 + 0.2f(t)$.

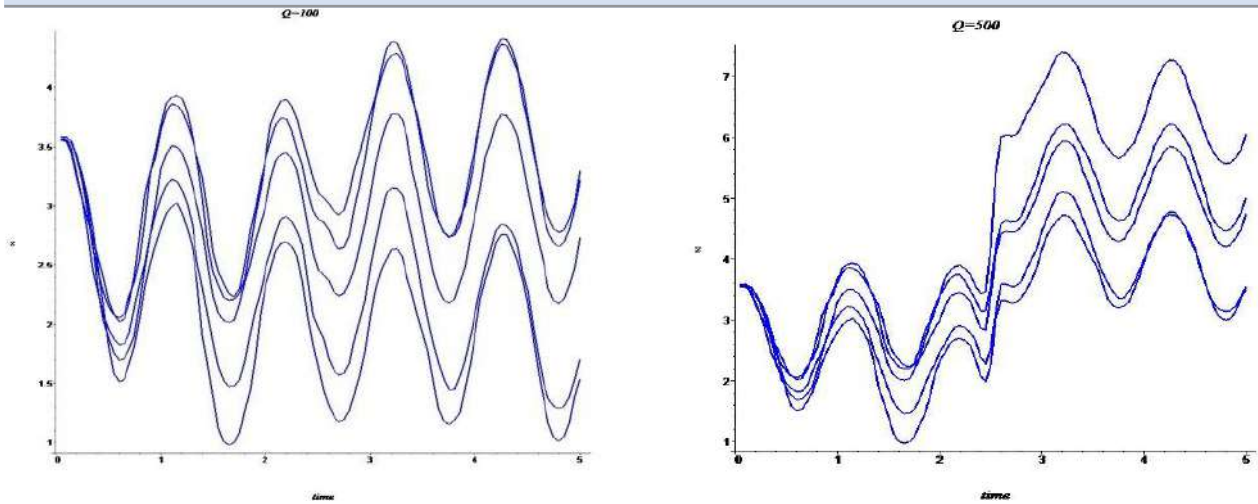


Figure 4. Solution of differential equation of motion (1) for $Q = 100$ and 500 . Here $z(0) = 3.5$, $v(0) = 0.8$, $a = -1.4 + 0.7f(t) + Qe^{-200(t-2.5)^2}$, $a_2 = 0.02 + 0.006f(t)$, $a_3 = -0.03 + 0.02f(t)$, $b = -80.2 + 40.1f(t)$, $w = 0.1 - 361\sin(6t - 0.45) + 40.4f(t)$, $c_2 = 0.3 + 0.2f(t)$, $c_3 = -0.2 + 0.1\sin(1.2t - 0.7) + 0.2f(t)$, $c_4 = 0.4 - 0.2\sin(1.1t - 0.26) + 0.2f(t)$, $c_5 = -0.2 + 0.05\sin(1.3t - 0.9) + 0.1f(t)$, $c_6 = -1.1 + 0.4f(t)$.

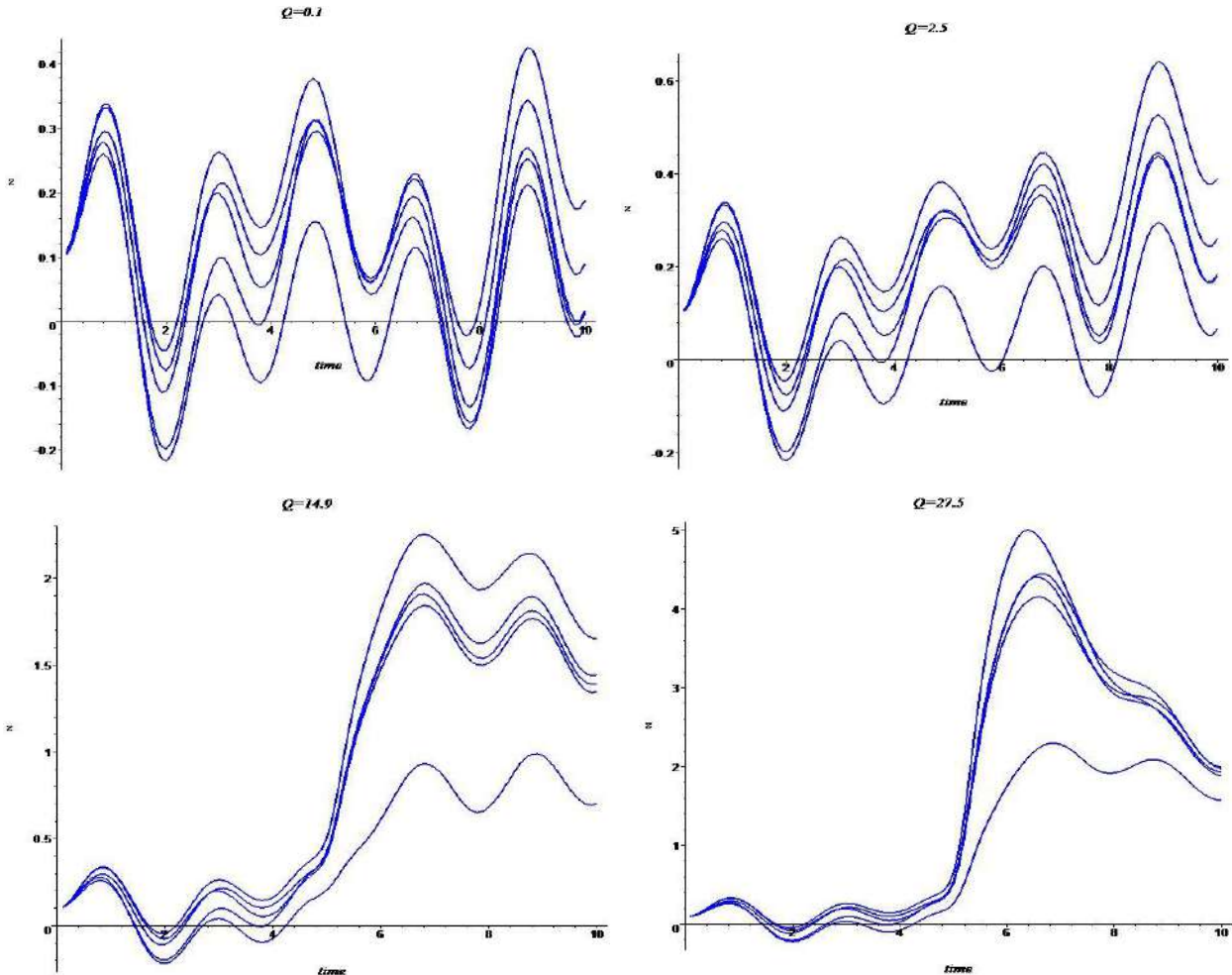


Figure 5. Solution of differential equation of motion (1) for $Q = 0.1, 2.5, 14.9$ and 27.5 . Here $z(0) = 0.1$, $v(0) = -0.02$, $a = -0.1 + 0.1f(t) + Qe^{-17(t-5)^2}$, $a_2 = 0.02 + 0.01\sin(1.5t - 1.4) + 0.007f(t)$, $a_3 = -0.03 + 0.002\sin(1.2t - 0.8) + 0.02f(t)$, $b = -1.5 + 0.01f(t)$, $w = 0.02 - 0.3\sin(2.5t - 1.7) + 0.01f(t)$, $c_2 = 1.5 + 0.4f(t)$, $c_3 = 0.1 + 0.1f(t)$, $c_4 = 0.1 + 0.2f(t)$, $c_5 = -0.1 + 0.1f(t)$, $c_6 = -0.1 + 0.05f(t)$.

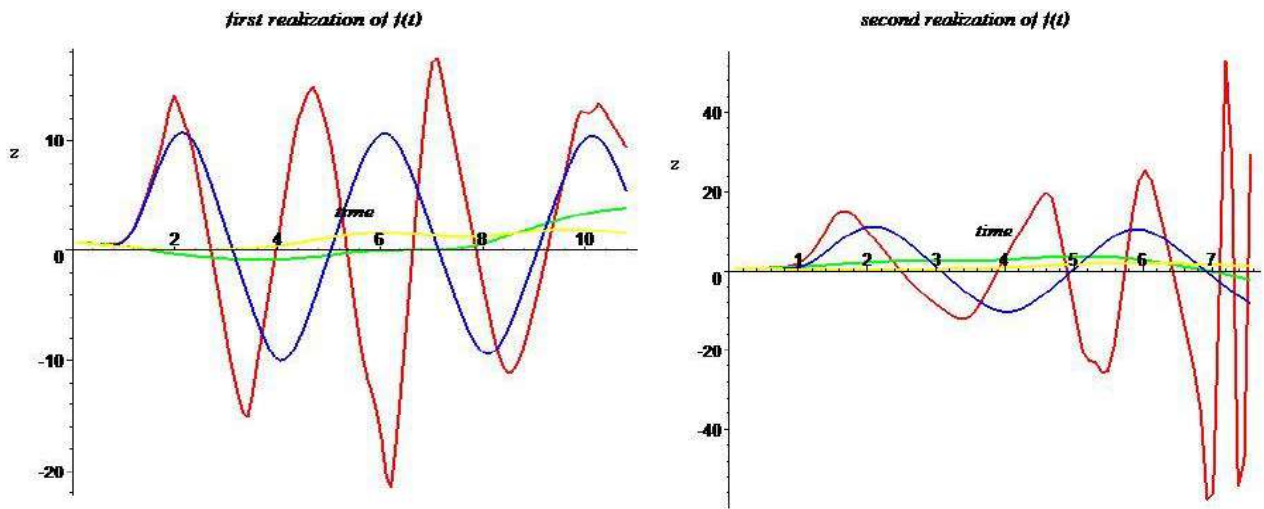


Figure 6. High maximum of a at $t = 1$ causes a large amplitude of $z(t)$ for $5 < t < 8$, if the level of stochasticity R is high enough; $Q = 1.4, R = 0.09$ (yellow), $Q = 28, R = 0.09$ (blue), $Q = 1.4, R = 0.9$ (green), $Q = 28, R = 0.9$ (red). Here $z(0) = 0.8, v(0) = -0.4, a = -0.2 + Rf(t) + Qe^{-17(t-1)^2}$,
 $a_2 = 0.04 + 0.1Rf(t), a_3 = -0.03 - 0.1Rf(t), b = -0.01 + Rf(t), w = 0.2 - Rf(t), c_2 = 0.2 + Rf(t),$
 $c_3 = -0.2 + Rf(t), c_4 = 0.3 + Rf(t), c_5 = -0.3 - Rf(t), c_6 = -0.1 + Rf(t).$

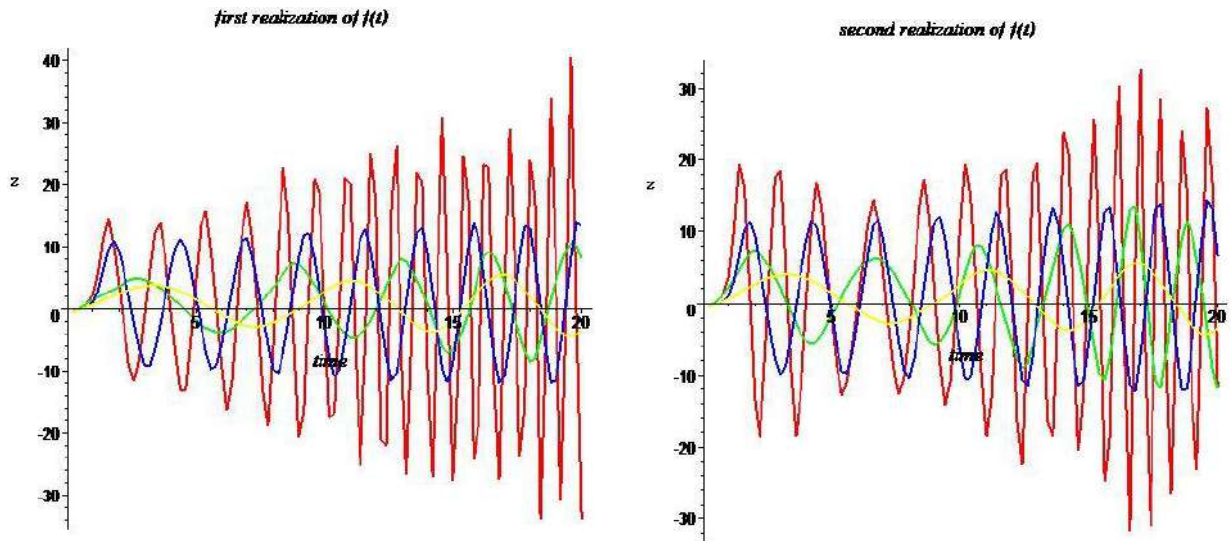


Figure 7. High maximum of a at $t = 1$ causes a large amplitude and frequency of $z(t)$ for $14 < t$, if the level of stochasticity R is high enough; $Q = 1.5, R = 0.09$ (yellow), $Q = 30, R = 0.09$ (blue), $Q = 1.5, R = 1.3$ (green),
 $Q = 30, R = 1.3$ (red). Here $z(0) = -0.8, v(0) = 1.5, a = -0.17 + Rf(t) + Qe^{-17(t-1)^2}$,
 $a_2 = 0.185 - 0.1Rf(t), a_3 = -0.075 - 0.01Rf(t), b = 0.04 + Rf(t), w = -0.1 + Rf(t), c_2 = -0.3 + Rf(t), c_3 =$
 $0.2 + Rf(t), c_4 = -0.2 + Rf(t), c_5 = 0.2 + Rf(t), c_6 = -0.23 + Rf(t).$

3. MEASURED TIME SERIES

Measured x_1, x_2, x_3, \dots we treat as coordinate of a particle of unit mass in discrete time. Then

$$v_{n+j} = x_{n+j} - x_{n+j-1}; n = 2,3,4, \dots, \\ 12; j = 0,1,2, \dots \quad (3)$$

has the role of velocity. We assume a certain form of acting force:

$$v_{n+j} - v_{n+j-1} = a(x_{n+j} - S) + a_2(x_{n+j} - S)^2 \\ + a_3(x_{n+j} - S)^3 + \\ + bv_{n+j} + w \\ + \sum_{i=2}^6 c_i \cos \frac{6.28(n+j)}{i}; \\ n = 3,4, \dots, 12 \quad (4)$$

where

$$S = \frac{1}{12} \sum_{n=1}^{12} x_{n+j}; j = 0,1,2, \dots \quad (5)$$

Ten force parameters (a, a_2, a_3, b, w, c_i) could be computed by solving ten equations (4), for $3 \leq n \leq 12$. We transform here, very accurately, the experimental data x_1, x_2, x_3, \dots to the force parameters as functions of discrete time j . This is a crucial difference in comparison with the Helbing and Zeithamer models [1,2,4], where force parameters are constants.

Look at an example. Measured data are $x_1 = 13.82, x_2 = 13.80, \dots, x_{27} = 13.52, x_{28} = 13.47, x_{29} = 13.45, x_{30} = 13.49, x_{31} = 13.46, \dots$

For $j = 28$, we find out $S = 13.59$ and force parameters $a = 4.88, a_2 = 3.45, a_3 = -141.64, b = 1.32, w = 0.02, c_2 = -0.096, c_3 = -0.11, c_4 = 0.08, c_5 = -0.29, c_6 = 0.29$.

For $j = 29$, results are $S = 13.62, a = -1.34, a_2 = 5.72, a_3 = -44.53, b = 1.63, w = 0.01, c_2 = 0.001, c_3 = -0.03, c_4 = -0.06, c_5 = 0.08, c_6 = 0.09$.

High maximum of the force parameter describing instability (a) announces a considerable change in the measured quantity.

This approach applies to different data – gross domestic product, stock market index [6], forced RLC circuit oscillations, variable star data, double pendulum data, earthquakes, electroencephalography, sea surface temperature anomaly, ...

4. LABORATORY EARTHQUAKE

Variation of the physical properties of tectonic faults is a very important subject in seismology. David Bolton investigates acoustic signals from the fault zone as precursors of laboratory earthquakes, performing friction experiments showing repetitive stick-slip failure. He observes a sample in the biaxial shear apparatus containing strain-gauge load cells, direct-current displacement transformers and piezoceramic sensors. Components of the sample are two gouge layers placed between three steel loading platens [7,8].

Using data from experiments with a biaxial deformation apparatus, we find out maxima of the force parameter a preceding big changes in the time series (figure 8-10).

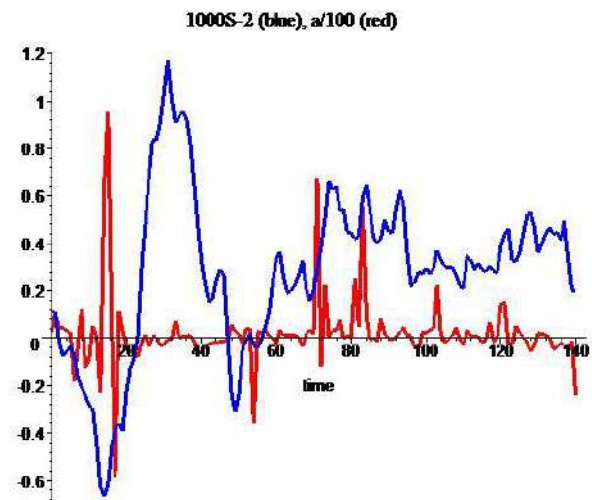


Figure 8. High maximum of the force parameter a (red) announces large increasing of voltage (blue). Considered time series is an electric output from the piezoelectric disk under mechanical shocks (experiment p2394) [8].

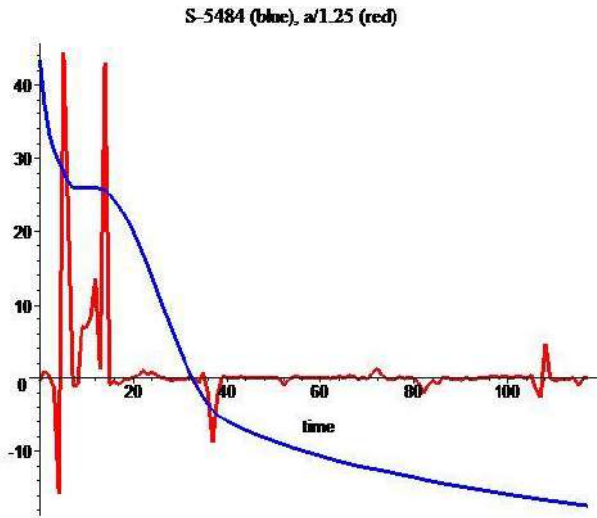


Figure 9. Two high maxima of the force parameter a (red) announce large decreasing of S (blue) (experiment p4677) [8].

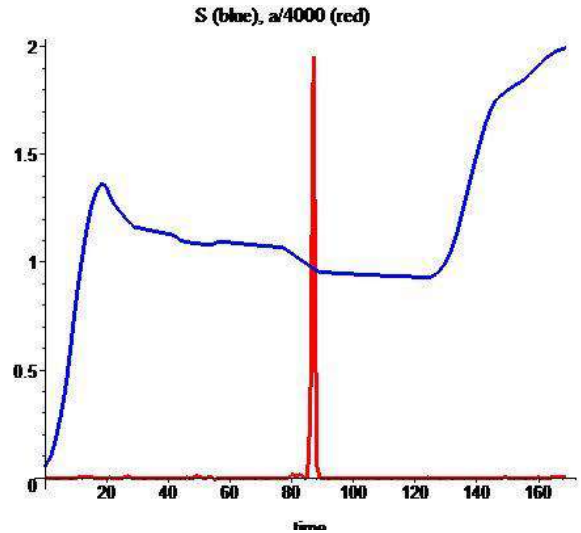


Figure 10. High maximum of the force parameter a (red) announces large increasing of S (blue) (experiment p4581) [8].

5. ANNUAL AVERAGE GLOBAL TEMPERATURE

Instability is a key feature of the climate system – its variability is strongly affected by small changes in natural and anthropogenic forcing [9]. The annual average global temperature is higher now than it has been for at least 12000 years [10,11]. The actual effects of climate change have not yet been sufficiently explored. Greenhouse gases are unlikely to be the only cause of rising temperatures and global warming. In 1883, a large eruption of the Krakatoa volcano occurred. It was the deadliest and most aggressive eruption of a volcano ever recorded

in history. The effects of this volcanic eruption were immediate but there are certainly far-reaching consequences. The year following the eruption, average Northern Hemisphere summer temperatures fell by $0.4\text{ }^{\circ}\text{C}$ ($0.72\text{ }^{\circ}\text{F}$).

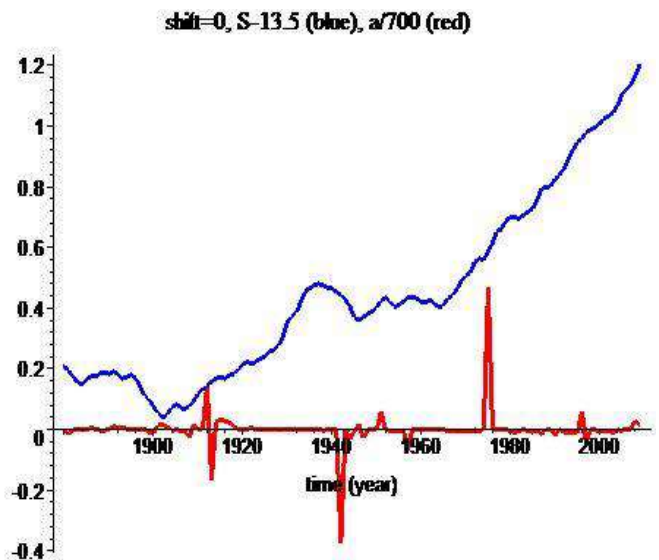
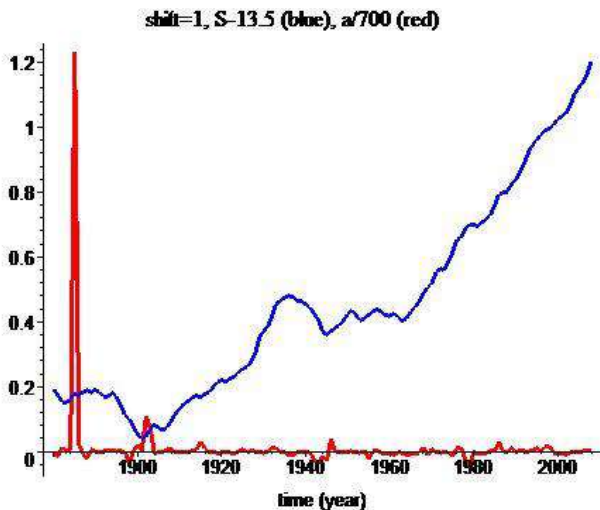


Figure 11. Left: large increase in global temperature (blue) [13] is preceded by a high maximum of the force parameter a (red). This maximum is probably related to the 1883 eruption of Krakatoa. Right: high maximum of the force parameter a (red) is probably related to the jump in the growth rate of carbon emissions from 1950 to 1970. [14]. We consider data $x_{i+\text{shift}}$ ($i = 1,2,3, \dots$) with $\text{shift} = 1$ (left) and $\text{shift} = 0$ (right).

There are also water years and record rainfall values recorded in California after the eruption [12]. The high maximum of the force parameter a

announces a large increase in global temperature. Besides greenhouse gases, Krakatoa 1883 eruption is a possible cause of modern global warming (figure 11,12).

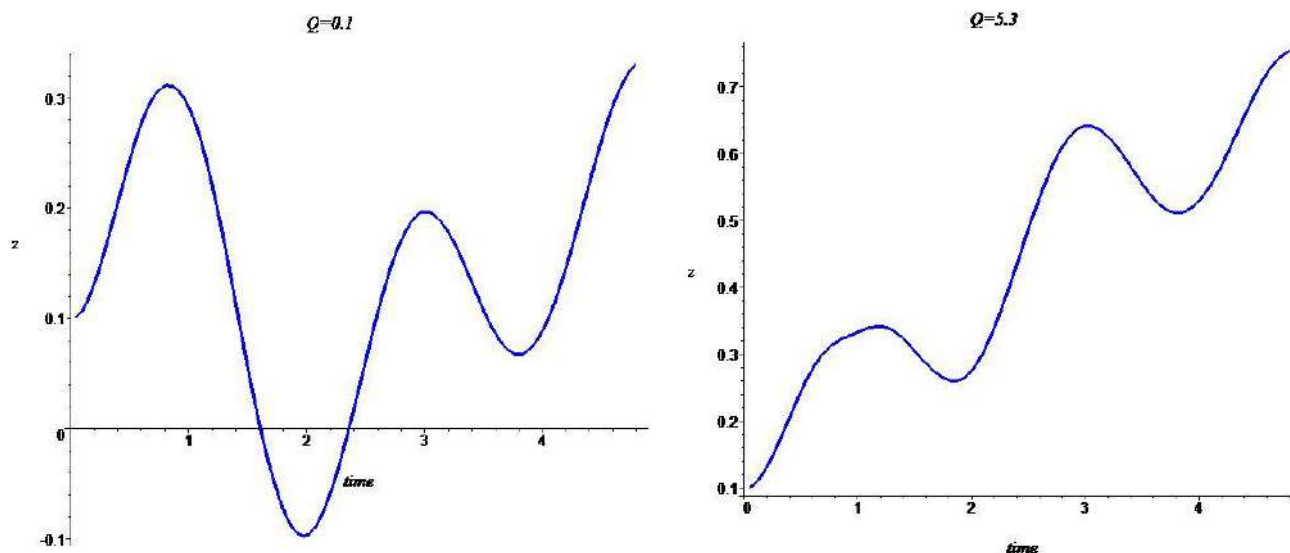


Figure 12. Simulation of global warming with differential equation

(1). If $Q = 0.1$, $z(4.8) = 0.34$, but $z(4.8) = 0.76$ for $Q = 5.3$.

Here $z(0) = 0.1$, $v(0) = -0.02$, $a = -0.1 + 0.1f(t) + Qe^{-17(t-1)^2}$,

$a_2 = 0.02 + 0.01\sin(1.5t - 1.4) + 0.007f(t)$,

$a_3 = -0.03 + 0.002\sin(1.2t - 0.8) + 0.02f(t)$, $b = -1.5 + 0.01f(t)$,

$w = 0.02 - 0.3\sin(2.5t - 1.7) + 0.01f(t)$, $c_2 = 1.5 + 0.4f(t)$, $c_3 = 0.1 + 0.1f(t)$,

$c_4 = 0.1 + 0.2f(t)$, $c_5 = -0.1 + 0.1f(t)$, $c_6 = -0.1 + 0.05f(t)$.

6. CONCLUSION

Considering stochastic and chaotic artificial time series, we found out that large instability in a short time interval causes large uncertainty, amplitude and frequency of future oscillations. For a measured time series, we compute the appropriate force using Newton's second law. The force acts on point in the space of data. Transformation of experimental data to the time-depending force parameters is a kind of information filtering. Then we can find out certain short time intervals with high instabilities and compare these heights. High maxima of the force parameter describing instability announce large changes in the measured quantities in mechanical experiments and a large increase in annual average global temperature. Besides greenhouse gases, the Krakatoa 1883 eruption is a possible cause of modern global warming.

7. REFERENCES

- [1] D. Helbing, P. Molnar and F. Schweitzer, *Computer Simulations of Pedestrian Dynamics and Trail Formation*, Conference Proceedings "Evolution of Natural Structures" Stuttgart 1994, 229–234.
- [2] C. Castellano, S. Fortunato and V. Loreto, *Statistical physics of social dynamics*, Rev. Mod. Phys., Vol. 81 (2009) 591–646.
- [3] F. Schweitzer, *Sociophysics*, Physics Today, Vol. 71 (2018) 40–46.
- [4] T.R. Zeithamer, *Economic Phenomena from the Viewpoint of the Mechanics of Materials*, Procedia – Social and Behavioral Sciences, Vol. 55 (2012) 547–553.
- [5] Z. Rajilić, N. Stupar, T. Vujičić and S. Lekić, *Emergence of ordered motion of the oscillator driven by fluctuating force*, Contemporary Materials, Vol. 11 (2020) 122–127.

[6] Z. Rajilić, N. Stupar and D. Malivuk Gak, *Mechanical Analysis of the S&P 500 Index Time Series*, Journal of Physics: Conference Series, Vol. 1814 (2021) 012004.

[7] D. C. Bolton, P. Shokouhi, B. Rouet-Leduc, C. Hulbert, J. Rivière, C. Marone and P. A. Johnson, *Characterizing Acoustic Signals and Searching for Precursors during the Laboratory Seismic Cycle Using Unsupervised Machine Learning*, Seismological Research Letters, Vol. 90 (2019) 1088–1098.

[8] D. C. Bolton, Penn State Rock Mechanics Lab, *Mechanical Data, experiments p2394 and p4677*, sites.psu.edu/cha-sbolton/2018/10/20/mechanical-data.

[9] M. Ghil and V. Lucarini, *The physics of climate variability and climate change*, Rev. Mod. Phys., Vol. 92 (2020) 035002.

[10] P. Voosen, *Global temperatures in 2020 tied record highs*, Science, Vol. 371 (2021) 334–335.

[11] S. Bova, Y. Rosenthal, Z. Liu, S.P. Godad and M. Yan, *Seasonal origin of the thermal maxima at the Holocene and the last interglacial*, Nature, Vol. 589 (2021) 548–553.

[12] R. S. Bradley, *The explosive volcanic eruption signal in northern hemisphere continental temperature records*, Climatic Change, Vol. 12 (1988) 221–243.

[13] National Oceanic and Atmospheric Administration, *History of global surface temperature since 1880*, www.ncdc.noaa.gov; European Environment Agency, *Global and European Temperature*, www.eea.europa.eu/data-and-maps/indicators/global-and-european-temperature/global-and-european-temperature-assessment-5; NASA, *Global Climate Change*, climate.nasa.gov.

[14] Global Carbon Emissions from Fossil Fuels, www.epa.gov/ghgemissions/global-greenhouse-gas-emissions-data.

ГРУБО ПРЕДВИЂАЊЕ ОСЦИЛАЦИЈА РАЧУНАЊЕМ МАКСИМАЛНЕ НЕСТАБИЛНОСТИ

Сажетак: Користимо други Њутнов закон кретања претпостављајући комбинацију хаоса и стохастике. За измјерени временски низ може се израчунати одговарајућа сила и на основу тога имати боље разумијевање посматраног комплексног система као и грубо предвиђати његово понашање. Од највећег је значаја параметар силе који описује нестабилност. Разматрамо неколико механичких експеримената и средњу глобалну температуру.

Кључне ријечи: хаос, стохастика, нестабилност, земљотрес, глобална температура.

Paper received: 10 September 2021

Paper accepted: 1 April 2022
